Chemistry–A European Journal
Research Article
doi.org/10.1002/chem.202400857
Chemistry Europe
European Chemical Societies Publishing
www.chemeurj.org

Graphene-Molecule Hybridization at a Ferromagnetic Interface

Iulia Cojocariu,*[a, b] Daniele Perilli,[c] Vitaliy Feyer,[d] and Matteo Jugovac*[b]

The introduction of a graphene (Gr) buffer layer between a ferromagnetic substrate and a metallorganic molecule is known to mediate the magnetic coupling between them, an effect attributed to a weak hybridization between graphene and molecule. In this paper, we present experimental evidence of this effect through a detailed investigation of the frontier electronic properties of iron phthalocyanine deposited on cobalt-supported graphene. Despite being physisorbed, the molecular adsorption on Gr/Co induces a sizeable charge transfer from graphene to the molecular macrocycle leading to the partial occupation of the LUMO and the appearance of an energetically localized hybrid state, which can be attributed to the overlap between the graphene p_z state and the molecular macrocycle. Graphene is not inert either; the adsorption of the molecule induces doping and alters the Fermi velocity of both the hybrid minicone state and the Dirac cone. Similar effects are observed when the molecular periphery is decorated with fluorine atoms, known for their electron-withdrawing properties, with minimal changes in the energy alignment.

1. Introduction

In the prospect of incorporating organic molecules into spintronic materials for information processing and storage, the control of magnetic moments, in both magnitude and direction, is of paramount importance. While molecules offer various advantages for spintronics, such as the ability to engineer them precisely through chemical synthesis,[1] the potential for large-scale nanometric reproducibility, and the possibility of functionalization through peripheral and axial ligand coordination,[2–6] a major challenge for their use in the spintronics field is stabilizing the magnetic moments of individual molecules against thermal fluctuations.

Since individual molecules' magnetic moments are relatively small, thermal energy usually exceeds typical magnetic energies even at temperatures far below ambient, leading to the disappearance of the thermal average of the magnetic moment and, consequently, the loss of any spin-dependent effect.[7] The immobilization of appropriate molecules, necessary for any form of device contacting, presents a second significant challenge: once immobilized on a solid surface through adsorption, the molecule-surface interaction dominates the molecule's electronic and magnetic properties, and it is not unusual for the desired functionality to be quenched.

A strategy for addressing the first challenge involves the use of molecular interactions with magnetically ordered substrates. Numerous experiments on metal-embedded porphyrins and phthalocyanines interfaced to ferromagnetic substrates have revealed a sizeable ferromagnetic response even at room temperature and without the need for an external magnetic field.[8–13] Density functional theory (DFT) calculations for these systems have shown that the observed ferromagnetic coupling is mediated by a 90° superexchange via the nitrogen atoms of the macrocycle core. Despite no overlap between the spin densities of equal sign of the ion in the molecule and the metal atoms in the substrate, the indirect 90° coupling via the spin density of the N atoms with the opposite signs is clearly visualized.

Moreover, phthalocyanine double deckers, where one rare-earth ion is coordinated by two parallel phthalocyanine (Pc) units, exhibit magnetic coupling to ferromagnetic Ni films,[14,15] Co films,[16] or Fe films as substrates,[17] with an opposite sign compared to planar transition-metal molecules. The opposite sign, antiferromagnetic instead of ferromagnetic, is attributed to the larger separation of the magnetic ion from the surface, altering the superexchange coupling path toward 180° compared to planarly coordinated transition metal ions.[14]

Relatedly, in particular cases, such as FePc on Gr/Co, magnetic coupling has been observed to change from ferromagnetic to antiferromagnetic by introducing a graphene buffer layer between the molecule and the ferromagnet.[18–20] The sp^2-hybridized carbon atoms in graphene are not expected to form covalent bonds with adsorbed molecules; instead, they

[a] I. Cojocariu
Dipartimento di Fisica, Università degli Studi di Trieste, Via A. Valerio 2, 34127 Trieste, Italy
E-mail: iulia.cojocariu@units.it
[b] I. Cojocariu, M. Jugovac
Elettra – Sincrotrone Trieste S.C.p.A, Basovizza S.S. 14, Km 163.5, 34149 Trieste, Italy
E-mail: matteo.jugovac@elettra.eu
[c] D. Perilli
Dipartimento di Scienza dei Materiali, Università degli Studi di Milano-Bicocca, via R. Cozzi 55, 20125 Milano, Italy
[d] V. Feyer
Peter Grünberg Institute (PGI-6), Forschungszentrum Jülich, Wilhelm-Johnen-Straße, 52428 Jülich, Germany

Supporting information for this article is available on the WWW under https://doi.org/10.1002/chem.202400857

are considered to be purely physisorbed on graphene. Although the relatively large distance between the molecule and the graphene carbon atoms,[21] which is comparable to the interlayer distance in molecular films, the graphene mediates the magnetic coupling between the molecules and the ferromagnetic film on which the graphene is grown.[20–24]

While the mediating role of graphene in the magnetic properties is well established, studies on electronic properties are limited and, until now, have been primarily focused on the ferromagnetic nickel substrate.

Within this framework, our manuscript aims at presenting a comprehensive study of the valence properties of the FePc/Gr/Co system through a combined experimental and theoretical investigation. Despite the weak interaction between the supported molecule and the hybrid Gr/Co system, considering the position of the HOMO and LUMO as well as the gap between them, the molecular states can not be regarded as electronically decoupled from the support. Our experimental findings reveal the presence of a hybrid state resulting from the overlap between the graphene p_z states and the organic component of the macrocycle (Pc). This hybridization was theoretically derived in previous work[21] focusing on the magnetism of the system but had never been experimentally observed, except indirectly through the magnetic coupling itself. Furthermore, this hybridization induces notable modifications in the electronic properties of graphene. We observe doping and Fermi velocity changes in both the Dirac cone and the graphene-cobalt hybrid state (minicone). Our study also demonstrates that the persistence of the hybrid state and the changes in graphene are unaffected by different degrees of halogenation of the periphery. A comparison of the FePc/Gr/Co and F_{16}FePc/Gr/Co systems, despite leading to a slightly different energy level alignment due to the varying work function of the interfaced molecule, reveals consistent results.

In conclusion, selecting the Gr/Co system as the support for molecule deposition proves to be highly advantageous for observing the hybrid state. This observation is hindered on Gr/Ni due to the energy overlap with the 3d nickel states.[25] Thus, our work contributes new insights into the electronic properties of this intriguing stacking, holding promise for room-temperature spintronics applications.

2. Results and Discussion

The supporting substrate comprises a monolayer of graphene grown on top of a 10 nm thick Co film deposited on clean W(110) using a well-established growth procedure,[26] detailed in the Methods section. The resulting graphene layer exhibits a (1×1) match with the substrate, as confirmed by low-energy electron diffraction (LEED). The close contact of graphene with cobalt significantly influences the magnetic and electronic properties of both materials.

Concerning the magnetic properties, the interaction induces a small magnetic moment on the carbon atoms, while the cobalt film undergoes substantial changes. The capping of thin cobalt films with graphene enhances the Co perpendicular magnetic anisotropy (PMA) and leads to the formation of exotic magnetic domain structures in ultrathin Co films with PMA up to a thickness of about 2 nm.[27,28] However, in thicker Co regimes, such as the one in this preparation, the magnetization of the film lies in the plane. The domains can be easily oriented along the easy magnetization axis due to the low coercive field of few tens of mT.[29]

Additionally, the contact of graphene to cobalt leads to significant deviations in the electronic structure compared to the freestanding case, creating a rich platform for functionalizing its electronic properties.[30–33] These changes are clearly visible in the energy *versus* momentum map of pristine Gr/Co, acquired at the $\overline{K}$ point of the first Brillouin zone, which is dominated by the main Dirac cone and the minicone near the Fermi level (see Figure 1a and b). The strong interaction between graphene and the underlying cobalt substrate is reflected in the shift of the main Dirac cone to higher binding energies and the formation of the minicone state.

This characteristic state arises from the orbital hybridization between Co 3d bands and graphene $2p_z$. Given the Co 3d bands involved in this hybridization are single spin-polarized, the newly formed state is also of a single-spin character.[34] By fitting the linear part of the main cone, the Dirac point apex is determined to be at 2.84 eV below the Fermi energy, with a Fermi velocity of 0.72×10^6 m/s, in line with previous reports.[30] Using an identical fitting procedure, we find the energy position of the minicone vertex to be 0.03 eV with a Fermi velocity of 1.25×10^5 m/s.

The deposition of a monolayer of FePc on Gr/Co induces several changes compared to the pristine interface, as evident in the energy *vs.* momentum map acquired at the $\overline{K}$ point (see Figure 1c and d). Notably, the graphene Dirac cone is shifted to lower binding energies, with its Dirac point now at 2.61 eV. This shift is accompanied by an increase in the Fermi velocity compared to the pristine case, reaching up to 0.81×10^6 m/s. Moreover, the presence of the molecule strongly affects the hybrid minicone state. By visual comparison of Figure 1a and d, it can be immediately noted that the minicone undergoes a shape modification from conical in pristine Gr/Co to parabolic-like upon adsorption of FePc on top. This is reflected in a shift in the minicone maximum to 0.07 eV and a strongly reduced Fermi velocity (0.80×10^5 m/s). Being the minicone a Co–C hybrid state, the charge transfer to the molecule affects the Gr–Co interfacial interaction and, hence, induces a shift in its energy position and a change of its E *vs.* $k_{//}$ dispersion.

The valence changes induced by molecular adsorption are readily observable also in the angle-integrated photoemission spectra. In Figure 2a, we compare the valence band spectra acquired at the $\overline{K}$ point of the first Brillouin zone for pristine Gr/Co and upon adsorption of a monolayer FePc.

Particularly noteworthy is a double peak feature centered at about 1.5 eV and a broad, intense molecular contribution in the 2.3–4.1 eV binding energy region. Additionally, the peak located at the Fermi level, attributed to the emission of Co 3d and the minicone state in pristine Gr/Co, undergoes a shift upon the adsorption of the molecule (refer to Figure 2b). Moreover, an additional state arises at around 0.85 eV.

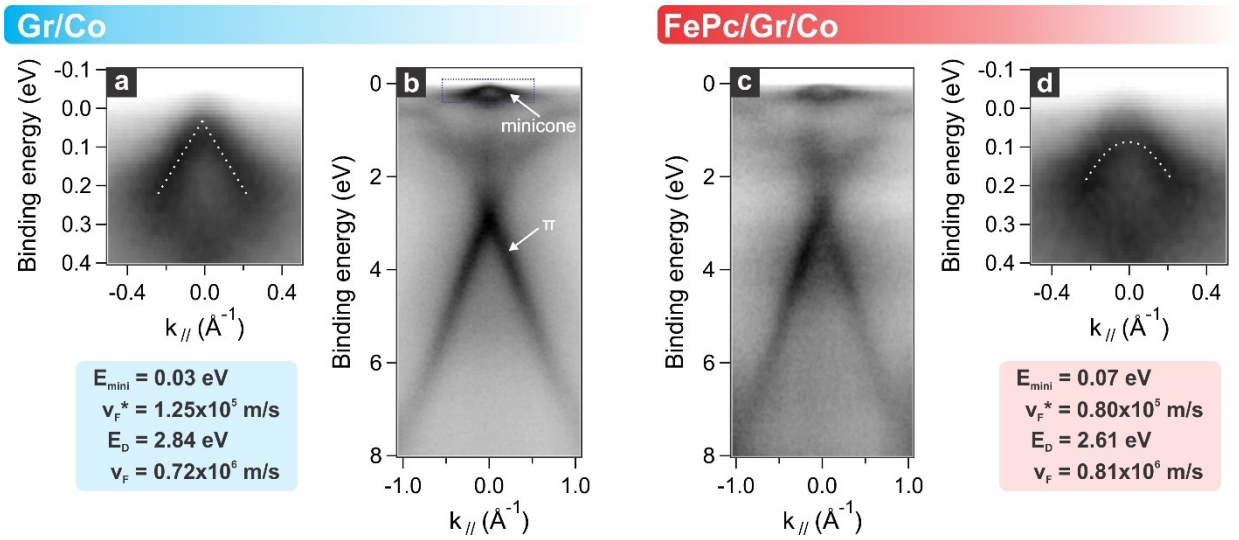

Figure 1. Comparison of the energy *vs.* momentum maps acquired at the $\overline{K}$ point (hv = 40 eV) before (a and b) and after (c and d) deposition of FePc on Gr/Co. b) and c) present the full energy region comprising the main Dirac cone and the minicone. a) and d) present the zoom of the region near the Fermi level where the minicone state is located. The corresponding values of Fermi velocity and the energy position of the maximum of minicone (v_F*, E_{mini}) and Dirac cone (v_F, E_D) are given in blue and red boxes for pristine Gr/Co and FePc/Gr/Co, respectively.

To gain a deeper understanding of these experimental results, we performed density functional theory (DFT) calculations using a model system, comprising a full monolayer of horizontally aligned FePc molecules positioned atop the Gr/Co interface (FePc/Gr/Co, see Figure 2c). We explored various stacking configurations for the molecule, with energy differences within ≈0.2 eV, and identified the most stable one, as illustrated in Figure 2c. In this configuration, the Fe atom is in a bridge position with respect to the C atoms of Gr, and the FePc–Gr distance is approximately 3.4 Å, suggesting a weak interaction. To unveil the electron interplay at the FePc/Gr/Co interface, we examined the electronic structure through the analysis of projected density of states (pDOS), as illustrated in Figure 2d. The DOS projected on the FePc molecule (bottom panel in Figure 2d) allows for identifying the energy position of the highest occupied molecular orbital (HOMO) and the lowest unoccupied molecular orbital (LUMO). The calculated HOMO matches the experimentally-determined value of 1.30 eV, while the HOMO-1, which has a strong Fe character, lies at 1.6 eV, consistent with the experiment. The energy position of the HOMO would suggest a weak electronic interaction between FePc and Gr/Co, additionally supported by the HOMO-LUMO gap, which remains almost unchanged for the adsorbed FePc as compared to the gas-phase one (1.44 *vs.* 1.46 eV); however, a charge transfer process takes place from Gr/Co to the molecule, as envisaged by the onset of the LUMO (see Figure 2e), which for the adsorbed FePc is located at the Fermi level. The calculated amount of charge transfer is computed to be 0.36 electrons for each molecule. It is interesting to highlight how this charge transfer originates from the coupling between the molecule's LUMO and the p_z system of Gr, similar to what seen by Casotto *et al.*[35] However, in this case, due to the pronounced n-type doping of graphene, there is the partial occupation of the LUMO.

It remains to unveil the nature of the new state, labelled with an asterisk, observed in the experimental valence band spectrum of Figure 2a, which is located between the HOMO and LUMO. The hybrid nature of this new state becomes more evident when examining the projected density of states (pDOS) onto the molecule and graphene, respectively (see Figure 2d and e). At the energy position where the state indexed by an asterisk is located, it is possible to observe an overlap between the molecular macrocycle and the p_z state of graphene (Figure 2e). The molecular nature of this state is also supported by the angular distribution in the photoemission map, being located at large $k_{//}$, in correspondence with the graphene's $\overline{K}$ point, and also compatible with the FePc's MOs angular distribution (see Figure S1 for the energy *vs.* momentum maps acquired along the $\overline{K\Gamma K'}$ direction of the first Brillouin zone relative to the Gr/Co system).[2] The hypothesis on its hybrid character is corroborated by comparison with the FePc/Gr/O/Co system, where a monolayer of FePc is deposited on top of oxygen-decoupled Gr/Co.[30] The intercalation of atomic oxygen is known to electronically decouple graphene from the substrate, lifting the strong interfacial hybridization. This ultimately leads to the quenching of the hybrid Gr–Co minicone state[30] and to the emptying of the Co 3d emission state at the Fermi energy (see Figure 2f). The valence band spectrum acquired after FePc deposition shows clear differences compared to the FePc/Gr/Co system. Indeed, oxygen intercalation clearly leads to the suppression of the charge transfer to the molecule. This effect is evidenced by the HOMO positioning, which locates at binding energies compatible with a fully decoupled.[25] The crucial role played by the Gr/Co platform in promoting the charge transfer to the molecule and the graphene-molecular hybridization is evidenced by the disappearance of the above-discussed hybrid state at equal molecular coverage. In this regard, it is to be emphasized that the

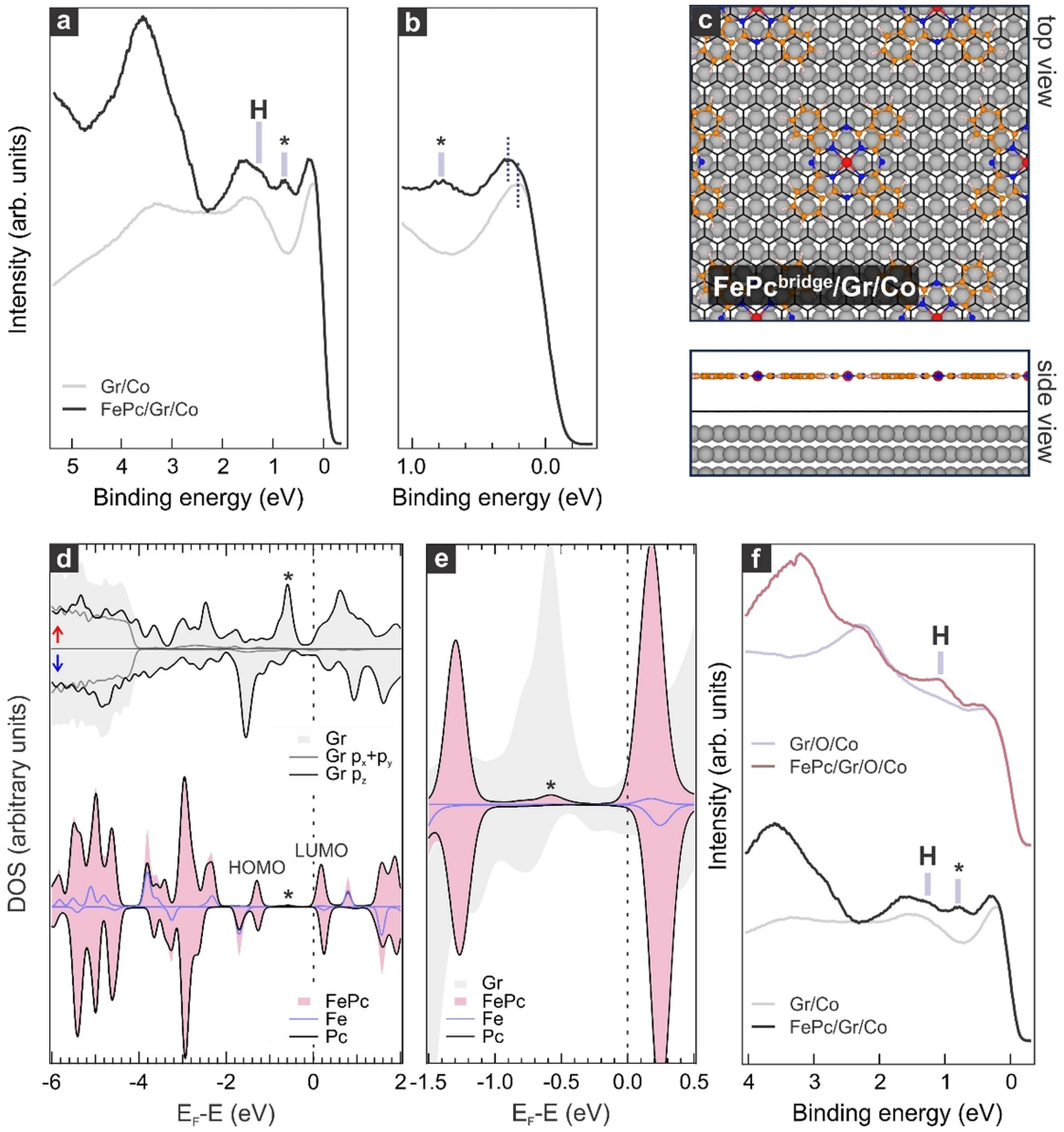

Figure 2. a) Valence band spectra acquired at the $\bar{K}$ point for the pristine Gr/Co (grey) and monolayer FePc/Gr/Co (black) interfaces. b) Zoom-in of the spectra in a) in the region near the Fermi level. c) Ball-and-stick model of DFT relaxed structures (side and top view) of FePc/Gr/Co interface. Color coding: grey–Co, black–graphene, red–iron, orange–carbon, blue–nitrogen, white–hydrogen. d) DFT projected DOS of the interface: graphene layer (top panel), FePc (bottom panel). H labels the state assigned to the Highest Occupied Molecular Orbital (HOMO) of the isolated molecule. The asterisk (*) indicates a new hybrid state formed between FePc and Gr. The two spin channels are marked with red (up) and blue (down) arrows. e) Zoom into the density of states projected onto the molecule in the energy range of −1.5 eV to +0.5 eV. f) Comparison of the valence band spectra acquired at the $\bar{K}$ point for monolayer FePc deposited on pristine and oxygen-intercalated Gr/Co.

very presence of this p_z state of graphene in the energy window under analysis is due to the strong hybridization between Co $3d_z^2$ and the out-of-plane component of graphene. As further confirmation of this, we present in Figure S2 the density of states calculated for the FePc/Gr system, computed based on the geometry of the FePc/Gr/Co system after removing the Co substrate. It is evident that the hybrid state between the HOMO and LUMO of the molecule is now completely absent. This underscores the essential role played by the Co substrate in the formation of this new FePc–Gr hybrid state. These observations clearly demonstrate the presence of vertical hybridization between graphene and cobalt and, consequently, between the molecular macrocycle and the graphene p_z system. The interlayer electronic hybridization supports the superexchange magnetic coupling path reported in previous works.[20,23]

The key role played by the organic component of the macrocycle (Pc) in the hybridization with Gr is further demonstrated by modifying the molecular peripheral *via* substitution with fluorine. As fluorine is a strongly withdrawing group, it is known to significantly affect the energy level alignment, by enhancing the electron-acceptor character of the molecular macrocycle.[4] This effect is clearly reflected in the experimental

work function (WF) changes. While the adsorption of FePc on Gr/Co was inducing a change in WF from 3.80 eV to 4.15 eV, the adsorption of F_{16}FePc leads the WF to be 4.45 eV, in accordance with the computed trend (Gr/Co–3.35 eV, FePc/Gr/Co–3.81 eV, F_{16}FePc/Gr/Co–4.14 eV). Despite these differences, the projected DOS on Gr does not exhibit a discernible difference when comparing the fluorinated case (top panel in Figure 3b) with the non-fluorinated case (top panel in Figure 2d). This is because fluorination increases the electron transfer to Gr by only 0.22 e^-, resulting in a negligible effect on the DOS of metallic system like Gr (strongly coupled with Co), as the extra electron charge is completely delocalized in the supercell. In line with theory, the experimental valence band spectra for monolayer F_{16}FePc on Gr/Co present a similar shape to the non-fluorinated case (see Figure 3a). The spectrum is characterized by a broad and intense molecular contribution located in the 4.2–2.4 eV range and a sharp state (labeled with an asterisk in Figure 3a) around 0.95 eV binding energy. Based on the position of the states in the pDOS by DFT calculations (Figure 3b), we propose that the experimental feature around 1 eV results from the contribution not only of this new molecular state mixed with Gr p_z bands but also of other states that we assigned to the highest energy molecular orbitals corresponding to the HOMO and next HOMO of the isolated FePc. All the molecular features result experimentally shifted by about 0.1 eV towards higher binding energy, consistently with a higher computed charge transfer from Gr/Co to F_{16}FePc induced by the electron-accepting macrocycle (0.36 e^-/FePc vs 0.58 e^-/F_{16}FePc). The intense state at 0.95 eV comprises the Gr-FePc hybrid state observed in the case of the non-fluorinated molecule. The persistence of the state regardless of fluorination, indicates that its presence is not influenced by inter-molecular interaction or peripheral repulsions but only governed by the vertical hybridization between the Gr/Co substrate and the macrocycle. Notably, the observed enhancement in experimental intensity of the interfacial state may reflect the higher charge transfer from Gr/Co to F_{16}FePc.

3. Conclusions

By employing a combined experimental and theoretical investigation based on angle-resolved photoemission and density functional theory calculations, respectively, we reveal that the introduction of graphene as a buffer layer between a molecular layer and a ferromagnetic substrate leads only to partial electronic decoupling of the molecule and the system is still affected by hybridization. The herein-reported study on FePc/Gr/Co and F_{16}FePc/Gr/Co showcases the presence of a hybrid interface state originating from the vertical interaction between the graphene's p_z state and the molecular macrocycle, regardless of the molecular periphery. We demonstrate that its persistence is a consequence of the strong interaction between the graphene monolayer and the ferromagnetic substrate, as lifting the Gr–Co interaction causes it to disappear. The interaction between the molecular layer and graphene also impacts the electronic properties of the latter, leading to energy shifts and Fermi velocity modifications of the graphene bands.

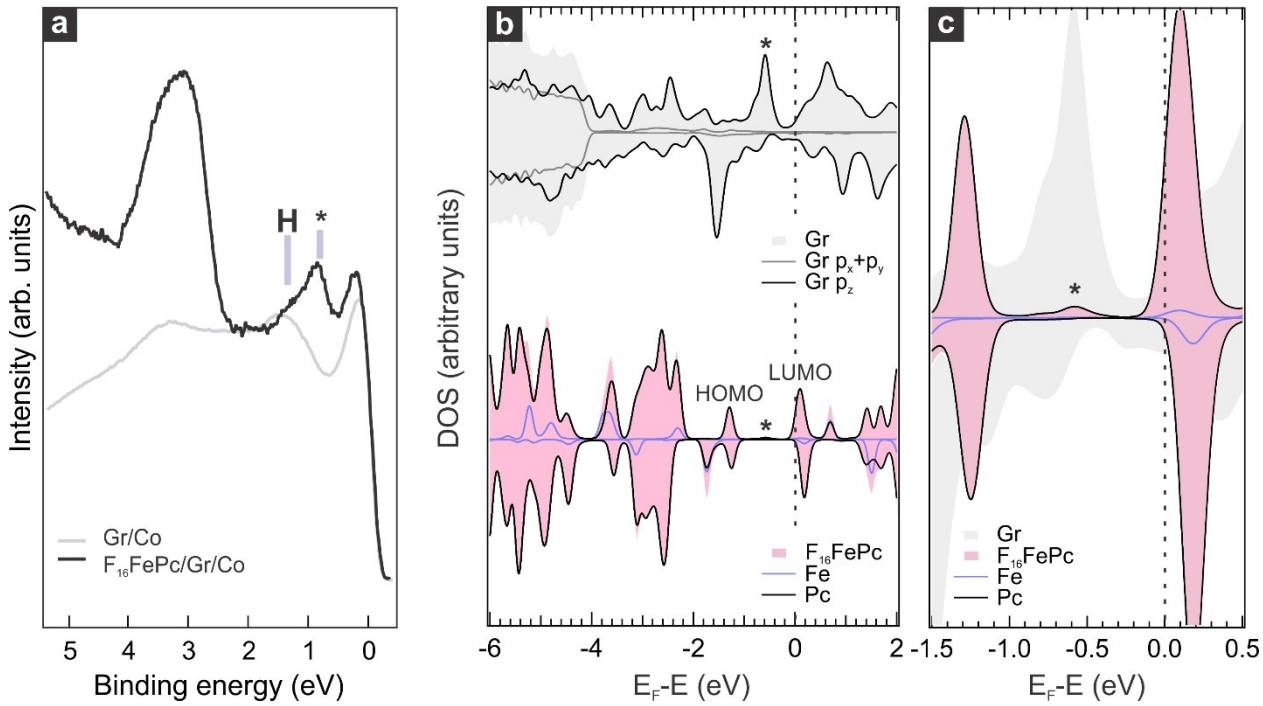

Figure 3. a) Valence band spectra acquired at the $\bar{K}$ point for the pristine Gr/Co (grey) and for monolayer F_{16}FePc/Gr/Co (black) interfaces. d) DFT projected DOS of the interface: graphene layer (top panel), F_{16}FePc (bottom panel). H labels the state assigned to the Highest Occupied Molecular Orbital (HOMO) of the isolated molecule. The asterisk (*) indicates a new hybrid state formed between F_{16}FePc and Gr. e) Zoom-in of the density of states projected onto the molecule in the energy range of −1.5 eV to +0.5 eV.

The findings here are particularly important in the field of spintronics, where Gr/ferromagnet interfaces have been recently introduced as a platform for stabilizing molecular magnetic ordering at room temperature. Indeed, it proved that the FePc–Gr/Co electronic hybridization can be experimentally visualized, and a magnetic superexchange path based on it is persuasive.

Experimental Section/Methods

Experimental Methods

The substrate for graphene growth is a 10 nm thick cobalt film deposited on clean W(110). On this surface, cobalt grows in an hcp crystalline arrangement, exposing the (0001) surface plane. Graphene is synthesized via ethylene (C_2H_4) chemical vapor deposition ($p = 5\times10^{-7}$ mbar), while keeping the sample at 800 K, which leads to the appearance of several graphene rotational domains. The conversion to an epitaxial (1×1) arrangement is achieved by annealing the sample up to 900 K while backfilling the experimental chamber with ethylene, taking advantage of the carbon dissolution and recondensation process.[26] The molecules were thermally sublimated at 680 K (FePc) and 700 K (F_{16}FePc) from a homemade Knudsen cell type evaporator onto the substrate kept at room temperature. The calibration of the molecular layer is performed using low-energy electron diffraction (LEED), by depositing the molecules on top of an Ag(100) crystal until the characteristic sharp LEED pattern was observed.[36] In all the experiments, the base pressure of the preparation and analysis chambers was below 2×10^{-10} mbar.

All the experiments were performed at the NanoESCA beamline of the Elettra synchrotron in Trieste (Italy), using a photoemission electron microscope (PEEM) operating in reciprocal space mode (k-PEEM).[37] The sample is illuminated with soft X-rays from the beamline equipped with two Apple-II type undulators, allowing for obtaining over a range from 40 to 1300 eV with variable polarizations: linear horizontal, linear vertical, or elliptical. The kinetic energy of the photoelectrons is selected by applying a bias voltage to the sample. The photoemitted electrons are collected by an optical column, energy-filtered in the double-hemispherical configuration (IDEA), and finally projected onto a 2D detector. All the measurements were performed at 90 K using p-polarized (perpendicular to the sample surface) incoming light with photon energy 35 eV, if not stated otherwise.

Theoretical Simulations

Density Functional Theory (DFT) calculations have been carried out using the plane-wave-based Quantum ESPRESSO package (QE).[38,39] The ultrasoft pseudopotentials have been adopted to describe the electron-ion interactions with C (2 s, 2p), N (2 s, 2p), H (1 s), F (2 s, 2p), Fe (4 s, 3d) and Co (4 s, 3d) treated as valence electrons.[40] Energy cutoffs of 46 and 326 Ry (for kinetic energy and charge density expansion, respectively) have been adopted for all calculations. During geometry optimization, a convergence criterion of 0.026 eV/Å for forces and 10^{-6} Ry for total energy was applied. The Perdew-Burke-Ernzerhof functional (PBE) was employed for electron exchange-correlation,[41] and van der Waals interactions were considered using the DFT–D3 formalism.[42] A U value[43] of 4.4 eV on Fe was applied across all calculations, consistent with prior literature recommendations.[44,45] To verify our setup, we computed and analyzed the ground state of an isolated FePc molecule in the gas-phase. We found a triplet state featuring two unpaired electrons in Fe d-orbitals and the HOMO and LUMO orbitals spatially localized on the organic part (Pc) of the FePc molecule (Figure S5). These findings match previous theoretical and experimental studies, confirming our setup's accuracy.[20,44,46]

The Co(0001) surface was modelled by a three-layer slab model with the two bottom layers fixed to bulk positions during geometry relaxation to simulate a semi-infinite solid. Converge tests by varying the number of Co layers and k-points mesh were conducted on the Gr/Co unit cell to check the computational parameters chosen for this study. Specifically, our computational setup (including k-grid, basis set cut off, vacuum spacing) accurately reproduces the geometric and electronic structure of this interface, including electron charge transfer from Co to Gr, magnetic moment on Co atoms, hybridization between Gr and Co states, and minicone features (see Figure S3 illustrating the projected band structure for the Gr/Co system testing a different number of Co layers (3 vs 6) and different k-points mesh (18×18 vs 24×24)). To simulate the Co(0001)-supported epitaxial graphene interface (Gr/Co) in the top-fcc registry, we utilized a (7×7) graphene cell on a (7×7) Co(0001) surface. A Monkhorst-Pack[47] k-Points mesh of $3\times3\times1$ and $9\times9\times1$ was used for the geometry relaxation and density of states (DOS) evaluation, respectively. To prevent interactions between adjacent periodic images, we included a vacuum space of 16.5 Å along the z-direction in the supercell model, along with a dipole correction. We confirmed the lack of interaction between replica images along the vacuum by plotting the electrostatic potential of Gr/Co and FePc/Gr/Co systems along the z-direction (Figure S4). We observed a flat potential between repeating images, indicating the absence of any interaction along the vacuum.

Acknowledgements

D.P. acknowledges funding from the European Union – NextGenerationEU through the Italian Ministry of University and Research under PNRR-M4C2I1.4 ICSC – Centro Nazionale di Ricerca in High Performance Computing, Big Data and Quantum Computing (Grant No. CN00000013). D.P. is grateful to Cristiana Di Valentin for useful discussions. Open Access publishing facilitated by Elettra Sincrotrone Trieste SCpA, as part of the Wiley - CRUI-CARE agreement.

Conflict of Interests

The authors declare no conflict of interest.

Data Availability Statement

The data that support the findings of this study are available from the corresponding author upon reasonable request.

Keywords: Graphene · Molecular electronics · Interfaces · Phthalocyanines

[1] E. Coronado, *Nat. Rev. Mater.* **2019**, *5*, 87.

[2] I. Cojocariu, S. Carlotto, H. M. Sturmeit, G. Zamborlini, M. Cinchetti, A. Cossaro, A. Verdini, L. Floreano, M. Jugovac, P. Puschnig, C. Piamonteze, M. Casarin, V. Feyer, C. M. Schneider, *Chem. A Eur. J.* **2021**, *27*, 3526.
[3] I. Cojocariu, S. Carlotto, G. Zamborlini, M. Jugovac, L. Schio, L. Floreano, M. Casarin, V. Feyer, C. M. Schneider, *J. Mater. Chem. C* **2021**, *9*, 12559.
[4] I. Cojocariu, M. Jugovac, S. Sarwar, J. Rawson, S. Sanz, P. Kögerler, V. Feyer, C. M. Schneider, *Adv. Funct. Mater.* **2022**, *32*, 2208507.
[5] H. M. Sturmeit, I. Cojocariu, A. Windischbacher, P. Puschnig, C. Piamonteze, M. Jugovac, A. Sala, C. Africh, G. Comelli, A. Cossaro, A. Verdini, L. Floreano, M. Stredansky, E. Vesselli, C. Hohner, M. Kettner, J. Libuda, C. M. Schneider, G. Zamborlini, M. Cinchetti, V. Feyer, *Small* **2021**, *17*, 2104779.
[6] I. Cojocariu, S. Carlotto, D. Baranowski, M. Jugovac, L. Schio, L. Floreano, M. Casarin, V. Feyer, C. M. Schneider, *Inorg. Chim. Acta* **2023**, *556*, 121657.
[7] W. Kuch, M. Bernien, *J. Phys. Condens. Matter* **2017**, *29*, 023001.
[8] A. Scheybal, T. Ramsvik, R. Bertschinger, M. Putero, F. Nolting, T. A. Jung, *Chem. Phys. Lett.* **2005**, *411*, 214.
[9] H. Wende, M. Bernien, J. Luo, C. Sorg, N. Ponpandian, J. Kurde, J. Miguel, M. Piantek, X. Xu, P. Eckhold, W. Kuch, K. Baberschke, P. M. Panchmatia, B. Sanyal, P. M. Oppeneer, O. Eriksson, *Nat. Mater* **2007**, *6*, 516.
[10] S. Javaid, M. Bowen, S. Boukari, L. Joly, J.-B. Beaufrand, X. Chen, Y. J. Dappe, F. Scheurer, J.-P. Kappler, J. Arabski, W. Wulfhekel, M. Alouani, E. Beaurepaire, *Phys. Rev. Lett.* **2010**, *105*, 077201.
[11] C. Wäckerlin, D. Chylarecka, A. Kleibert, K. Müller, C. Iacovita, F. Nolting, T. A. Jung, N. Ballav, *Nat. Commun.* **2010**, *1*, 61.
[12] D. Chylarecka, T. K. Kim, K. Tarafder, K. Müller, K. Gödel, I. Czekaj, C. Wäckerlin, M. Cinchetti, M. E. Ali, C. Piamonteze, F. Schmitt, J.-P. Wüstenberg, C. Ziegler, F. Nolting, M. Aeschlimann, P. M. Oppeneer, N. Ballav, T. A. Jung, *J. Phys. Chem. C* **2011**, *115*, 1295.
[13] S. Bhandary, B. Brena, P. M. Panchmatia, I. Brumboiu, M. Bernien, C. Weis, B. Krumme, C. Etz, W. Kuch, H. Wende, O. Eriksson, B. Sanyal, *Phys. Rev. B* **2013**, *88*, 024401.
[14] A. Lodi Rizzini, C. Krull, T. Balashov, J. J. Kavich, A. Mugarza, P. S. Miedema, P. K. Thakur, V. Sessi, S. Klyatskaya, M. Ruben, S. Stepanow, P. Gambardella, *Phys. Rev. Lett.* **2011**, *107*, 177205.
[15] A. Lodi Rizzini, C. Krull, A. Mugarza, T. Balashov, C. Nistor, R. Piquerel, S. Klyatskaya, M. Ruben, P. M. Sheverdyaeva, P. Moras, C. Carbone, C. Stamm, P. S. Miedema, P. K. Thakur, V. Sessi, M. Soares, F. Yakhou-Harris, J. C. Cezar, S. Stepanow, P. Gambardella, *Surf. Sci.* **2014**, *630*, 361.
[16] D. Klar, S. Klyatskaya, A. Candini, B. Krumme, K. Kummer, P. Ohresser, V. Corradini, V. De Renzi, R. Biagi, L. Joly, J.-P. Kappler, U. Del Pennino, M. Affronte, H. Wende, M. Ruben, *Beilstein J. Nanotechnol.* **2013**, *4*, 320.
[17] C. Nistor, C. Krull, A. Mugarza, S. Stepanow, C. Stamm, M. Soares, S. Klyatskaya, M. Ruben, P. Gambardella, *Phys. Rev. B* **2015**, *92*, 184402.
[18] E. Annese, F. Casolari, J. Fujii, G. Rossi, *Phys. Rev. B* **2013**, *87*, 054420.
[19] E. Annese, G. Di Santo, F. Choueikani, E. Otero, P. Ohresser, *ACS Omega* **2019**, *4*, 5076.
[20] G. Avvisati, C. Cardoso, D. Varsano, A. Ferretti, P. Gargiani, M. G. Betti, *Nano Lett.* **2018**, *18*, 2268.
[21] C. F. Hermanns, K. Tarafder, M. Bernien, A. Krüger, Y. Chang, P. M. Oppeneer, W. Kuch, *Adv. Mater.* **2013**, *25*, 3473.
[22] A. Candini, V. Bellini, D. Klar, V. Corradini, R. Biagi, V. De Renzi, K. Kummer, N. B. Brookes, U. Del Pennino, H. Wende, M. Affronte, *J. Phys. Chem. C* **2014**, *118*, 17670.
[23] G. Avvisati, P. Gargiani, P. Mondelli, F. Presel, A. Baraldi, M. G. Betti, *Phys. Rev. B* **2018**, *98*, 115412.
[24] Y. Wang, Z. Wang, X. Li, *Phys. Rev. B* **2024**, *109*, 014428.
[25] W.-G. Ye, D. Liu, X.-F. Peng, W.-D. Dou, *Chinese Phys. B* **2013**, *22*, 117301.
[26] M. Jugovac, F. Genuzio, E. Gonzalez Lazo, N. Stojić, G. Zamborlini, V. Feyer, T. O. Menteş, A. Locatelli, C. M. Schneider, *Carbon* **2019**, *152*, 489.
[27] M. Blanco-Rey, P. Perna, A. Gudin, J. M. Diez, A. Anadón, P. Olleros-Rodríguez, L. de Melo Costa, M. Valvidares, P. Gargiani, A. Guedeja-Marron, M. Cabero, M. Varela, C. García-Fernández, M. M. Otrokov, J. Camarero, R. Miranda, A. Arnau, J. I. Cerdá, *ACS Appl. Nano Mater.* **2021**, *4*, 4398.
[28] F. Ajejas, A. Gudín, R. Guerrero, A. Anadón Barcelona, J. M. Diez, L. de Melo Costa, P. Olleros, M. A. Niño, S. Pizzini, J. Vogel, M. Valvidares, P. Gargiani, M. Cabero, M. Varela, J. Camarero, R. Miranda, P. Perna, *Nano Lett.* **2018**, *18*, 5364.
[29] J. E. Prieto, O. Krupin, S. Gorovikov, K. Döbrich, G. Kaindl, K. Starke, *Phys. Rev. B* **2005**, *72*, 092409.
[30] M. Jugovac, F. Genuzio, T. O. Menteş, A. Locatelli, G. Zamborlini, V. Feyer, C. M. Schneider, *Carbon* **2020**, *163*, 341.
[31] M. Jugovac, C. Tresca, I. Cojocariu, G. D. Santo, W. Zhao, L. Petaccia, P. Moras, G. Profeta, F. Bisti, *Phys. Rev. B* **2022**, *105*, L241107.
[32] M. Jugovac, I. Cojocariu, F. Genuzio, C. Bigi, D. Mondal, I. Vobornik, J. Fujii, P. Moras, V. Feyer, A. Locatelli, T. O. Menteş, *Adv. Elect. Mater.* **2023**, *9*, 2300031.
[33] M. Jugovac, I. Cojocariu, J. Sánchez-Barriga, P. Gargiani, M. Valvidares, V. Feyer, S. Blügel, G. Bihlmayer, P. Perna, *Adv. Mater.* **2023**, *35*, 2301441.
[34] M. Jugovac, E. D. Donkor, P. Moras, I. Cojocariu, F. Genuzio, G. Zamborlini, G. Di Santo, L. Petaccia, N. Stojić, V. Feyer, C. M. Schneider, A. Locatelli, T. O. Menteş, *Carbon* **2022**, *198*, 188.
[35] A. Casotto, G. Drera, D. Perilli, S. Freddi, S. Pagliara, M. Zanotti, L. Schio, A. Verdini, L. Floreano, C. Di Valentin, L. Sangaletti, *Nanoscale* **2022**, *14*, 13166.
[36] V. Feyer, M. Graus, P. Nigge, M. Wießner, R. G. Acres, C. Wiemann, C. M. Schneider, A. Schöll, F. Reinert, *Surf. Sci.* **2014**, *621*, 64.
[37] C. Wiemann, M. Patt, I. P. Krug, N. B. Weber, M. Escher, M. Merkel, C. M. Schneider, *e-J. Surf. Sci. Nanotechnol.* **2011**, *9*, 395.
[38] P. Giannozzi, S. Baroni, N. Bonini, M. Calandra, R. Car, C. Cavazzoni, D. Ceresoli, G. L. Chiarotti, M. Cococcioni, I. Dabo, A. Dal Corso, S. De Gironcoli, S. Fabris, G. Fratesi, R. Gebauer, U. Gerstmann, C. Gougoussis, A. Kokalj, M. Lazzeri, L. Martin-Samos, N. Marzari, F. Mauri, R. Mazzarello, S. Paolini, A. Pasquarello, L. Paulatto, C. Sbraccia, S. Scandolo, G. Sclauzero, A. P. Seitsonen, A. Smogunov, P. Umari, R. M. Wentzcovitch, *J. Phys. Condens. Matter* **2009**, *21*, 395502.
[39] P. Giannozzi, O. Andreussi, T. Brumme, O. Bunau, M. Buongiorno Nardelli, M. Calandra, R. Car, C. Cavazzoni, D. Ceresoli, M. Cococcioni, N. Colonna, I. Carnimeo, A. Dal Corso, S. De Gironcoli, P. Delugas, R. A. DiStasio, A. Ferretti, A. Floris, G. Fratesi, G. Fugallo, R. Gebauer, U. Gerstmann, F. Giustino, T. Gorni, J. Jia, M. Kawamura, H.-Y. Ko, A. Kokalj, E. Küçükbenli, M. Lazzeri, M. Marsili, N. Marzari, F. Mauri, N. L. Nguyen, H.-V. Nguyen, A. Otero-de-la-Roza, L. Paulatto, S. Poncé, D. Rocca, R. Sabatini, B. Santra, M. Schlipf, A. P. Seitsonen, A. Smogunov, I. Timrov, T. Thonhauser, P. Umari, N. Vast, X. Wu, S. Baroni, *J. Phys. Condens. Matter* **2017**, *29*, 465901.
[40] A. Dal Corso, *Comput. Mater. Sci.* **2014**, *95*, 337.
[41] J. P. Perdew, K. Burke, M. Ernzerhof, *Phys. Rev. Lett.* **1996**, *77*, 3865.
[42] S. Grimme, J. Antony, S. Ehrlich, H. Krieg, *J. Chem. Phys.* **2010**, *132*, 154104.
[43] B. Himmetoglu, A. Floris, S. De Gironcoli, M. Cococcioni, *Int. J. Quantum Chem.* **2014**, *114*, 14.
[44] I. E. Brumboiu, S. Haldar, J. Lüder, O. Eriksson, H. C. Herper, B. Brena, B. Sanyal, *J. Chem. Theory Comput.* **2016**, *12*, 1772.
[45] I. E. Brumboiu, S. Haldar, J. Lüder, O. Eriksson, H. C. Herper, B. Brena, B. Sanyal, *J. Phys. Chem. A* **2019**, *123*, 3214.
[46] B. Brena, C. Puglia, M. De Simone, M. Coreno, K. Tarafder, V. Feyer, R. Banerjee, E. Göthelid, B. Sanyal, P. M. Oppeneer, O. Eriksson, *J. Chem. Phys.* **2011**, *134*, 074312.
[47] H. J. Monkhorst, J. D. Pack, *Phys. Rev. B* **1976**, *13*, 5188.

Manuscript received: February 29, 2024
Accepted manuscript online: June 6, 2024
Version of record online: September 16, 2024